# *Ab initio* molecular treatment for charge transfer by $P^{3+}$ ions on hydrogen and helium

A. Moussa,[1] A. Zaidi,[1] S. Lahmar,[1] and M.-C. Bacchus-Montabonel[2]

[1]*Laboratoire de Spectrosopie Atomique, Moléculaire et Applications (LSAMA), Faculté des Sciences de Tunis, Université Tunis El Manar, Campus Universitaire, TN-1060 Tunis, Tunisia*

[2]*Laboratoire de Spectrométrie Ionique et Moléculaire, UMR 5579, CNRS et Université Lyon I, 43 Boulevard du 11 Novembre 1918, F-69622 Villeurbanne Cedex, France*

(Received 6 October 2009; published 17 February 2010)

A theoretical treatment of charge-transfer processes induced by collision of phosphorus $P^{3+}(3s^2)^1S$ ions on atomic hydrogen and helium has been carried out using *ab initio* potential-energy curves and couplings at the multireference configuration interaction level of theory. The cross sections calculated by means of semiclassical collision methods show the existence of a significant charge transfer in the 0.1–700-keV laboratory energy range. Radial and rotational coupling interactions were analyzed for both collision systems.

DOI: 10.1103/PhysRevA.81.022713 PACS number(s): 34.70.+e

## I. INTRODUCTION

Low-energy electron capture by multiply charged ions with atomic hydrogen and helium has been shown to be an important process in controlled thermonuclear fusion research as well as in astrophysical plasmas, in which emission lines are used to provide direct information on the ionization structure of astronomical objects [1,2]. Such reactions have been recognized to be possible ionization sources [3]. Considerable interest has been devoted to heavy ions of silicon, sulfur, and, more recently, phosphorus in order to obtain information on their interaction with particles or external fields. Phosphorus is a very important element in biological systems. Phosphorus ions are present also in astronomical media as planetary nebulae or diffuse interstellar media [4,5], and knowledge about reactions involving phosphorus may be of great interest in exobiology investigations on possible processes at the origin of life [6]. In that sense, recent theoretical studies have been undertaken on the $P + H^+$ [7] and $P^{2+} + H$ [8] charge-transfer processes at low to intermediate collision energies based on a molecular-expansion method.

In order to have a wider view on charge-transfer processes involving phosphorus ions, we have investigated two other systems, the $P^{3+}(3s^2)^1S + H$ and $P^{3+}(3s^2)^1S + He$ reactions. Their collision behavior may be compared to the $P^{2+}(3s^23p)^2P^o + H$ collision system we had studied previously [8]. The evaluation of the potential-energy curves and couplings of the different states involved in the process has been performed by means of *ab initio* quantum-chemistry molecular methods. Such molecular calculations have been followed by a semiclassical collision treatment in the 0.1- to 700-keV laboratory energy range. To our knowledge, only analytic fits of charge-exchange-rate coefficients [9] are available for these systems. The study has been performed for the ground-state $P^{3+}(3s^2)^1S + H$ and $P^{3+}(3s^2)^1S + He$ entry channels. The first metastable $P^{3+}(3s3p)^3P^o$ state lies 8.47822 eV above the ground-state $P^{3+}(3s^2)^1S$ ion, too high in energy for the $P^{3+}(3s3p)^3P^o + H$ charge-transfer process to compete with the $P^{3+}(3s^2)^1S + H$ one. Because spin-orbit effects may be neglected in the collision-energy range of interest, the corresponding $P^{3+}(3s3p)^3P^o + He\,^3\Pi$ entry channel cannot intervene in the $P^{3+}(3s^2)^1S + He$ process. The second metastable $P^{3+}(3s3p)^1P$ ion has even more energy, 13.04195 eV above the ground-state $P^{3+}(3s^2)^1S$ ion, and the $P^{3+}(3s3p)^1P + He$ reaction would not be considered in the calculation.

## II. MOLECULAR CALCULATIONS

The potential-energy curves have been determined using the MOLPRO suite of *ab initio* programs [10] at the state average complete active space self-consistent field–multireference configuation interaction (CASSCF-MRCI) level of theory. The active space includes the $n = 3$ and $n = 4$ (s,p,d) orbitals for the phosphorus element and the $1s$ orbital for hydrogen and helium. Calculations have been performed with the correlation-consistent sextuple $\zeta$ aug-cc-pV6Z basis sets of Woon and Dunning [11] for all atoms. The asymptotic energy levels are displayed in Tables I and II respectively for the $P^{3+}(3s^2)^1S + He$ and $P^{3+}(3s^2)^1S + H$ molecular systems. The asymptotic energies calculated using MRCI are in reasonable agreement with experimental data, with a discrepancy in the range of $1.1 \times 10^{-3}$ to $5.5 \times 10^{-3}$ a.u. [12]. The spin-orbit effects may be neglected in the collision-energy range of interest, so only singlet states have been considered for the $P^{3+}(3s^2)^1S + He$ collision system and doublet states for the $P^{3+}(3s^2)^1S + H$ one.

The radial coupling matrix elements between all pairs of states of the same symmetry have been calculated by means of the finite difference technique:

$$g_{KL}(R) = \langle\psi_K|\partial/\partial R|\psi_L\rangle = \langle\psi_K(R)|\lim_{\Delta\to 0}\frac{1}{\Delta}|\psi_L(R+\Delta) - \psi_L(R)\rangle. \quad (1)$$

Taking account of the orthogonality of the eigenfunctions $|\psi_K(R)\rangle$ and $|\psi_L(R)\rangle$for $K \neq L$, we reduce this to

$$g_{KL}(R) = \langle\psi_K|\partial/\partial R|\psi_L\rangle = \lim_{\Delta\to 0}\frac{1}{\Delta}\langle\psi_K(R)|\psi_L(R+\Delta)\rangle \quad (2)$$

with the parameter $\Delta = 0.0012$ a.u. and use the three-point numerical differentiation method for reasons of numerical accuracy [13].

The rotational coupling matrix elements $\langle\psi_K(R)|iL_y|\psi_L(R)\rangle$ between states of angular moment $\Delta\Lambda = \pm 1$

 

TABLE I. Comparison of asymptotic energy levels with experimental data (a.u.) for the $P^{3+}(3s^2)^1S + He$ system.

| | MRCI calculation | Experiment [12] |
|---|---|---|
| $P^{3+}(3s^2)^1S$ $+He(1s^2)^1S(^1\Sigma^+)$ | 0.2027 | 0.2038 |
| $P^{2+}(3s^23p)^2P^o$ $+He^+(1s)^2S(^1\Sigma^+, ^1\Pi)$ | 0.0 | 0.0 |

have been calculated directly from the quadrupole moment tensor between electronic wave functions from the expression

$$\langle\psi_K|iL_y|\psi_L\rangle = \langle\psi_K|\,x\frac{\partial}{\partial z} - z\frac{\partial}{\partial x}\,|\psi_L\rangle\,. \tag{3}$$

The evaluation of the quadrupole-moment-tensor elements also may lead to the consideration of translation effects in the collision dynamics. In the approximation of the common translation factor developed by Errea *et al.* [14], the radial and rotational coupling matrix elements between states $\psi_K$ and $\psi_L$ may indeed be transformed respectively into [15]

$$\begin{aligned}&\langle\psi_K|\partial/\partial R - (\varepsilon_K - \varepsilon_L)z^2/2R|\psi_L\rangle,\\ &\langle\psi_K|iL_y + (\varepsilon_K - \varepsilon_L)zx|\psi_L\rangle,\end{aligned} \tag{4}$$

where $\varepsilon_K$ and $\varepsilon_L$ are the electronic energies of states $\psi_K$ and $\psi_L$ and where $z^2$ and $zx$ are the components of the quadrupole moment tensor. This expression is applicable for any choice of electronic coordinates. The phosphorus nucleus has been chosen as origin of electronic coordinates.

The $P^{3+}(3s^2)^1S + He$ collision system is relatively simple, with only the $P^{2+}(3s^23p)^2P^o + He^+(1s)^2S$ charge-transfer exit channel accessible in the $^1\Sigma^+$ and $^1\Pi$ symmetries. As pointed out in the introduction, the first metastable $P^{3+}(3s3p)^3P^o$ ion would lead to a $^3\Pi\{P^{3+}(3s3p)^3P^o + He\}$ entry channel and the second metastable $P^{3+}(3s3p)^1P$ has far too much energy to compete with the ground-state $P^{3+}(3s^2)^1S + He$ entry channel. Thus, only three states have to be taken into account in the collision process: the entry channel $^1\Sigma^+\{P^{3+}(3s^2)^1S + He\}$ and the $^1\Sigma^+$, $^1\Pi\{P^{2+}(3s^23p)^2P^o + He^+(1s)^2S\}$ levels. The potential-energy curves are presented in Fig. 1; the corresponding radial and rotational coupling matrix elements are displayed respectively in Figs. 2 and 3. The potentials show clearly around 10 a.u. a very sharp avoided crossing between the entry channel and the $^1\Sigma^+\{P^{2+}(3s^23p)^2P^o + He^+(1s)^2S\}$ capture channel. Such avoided crossing is evidenced also on the radial coupling matrix element, which appears extremely peaked, 25.39 a.u.

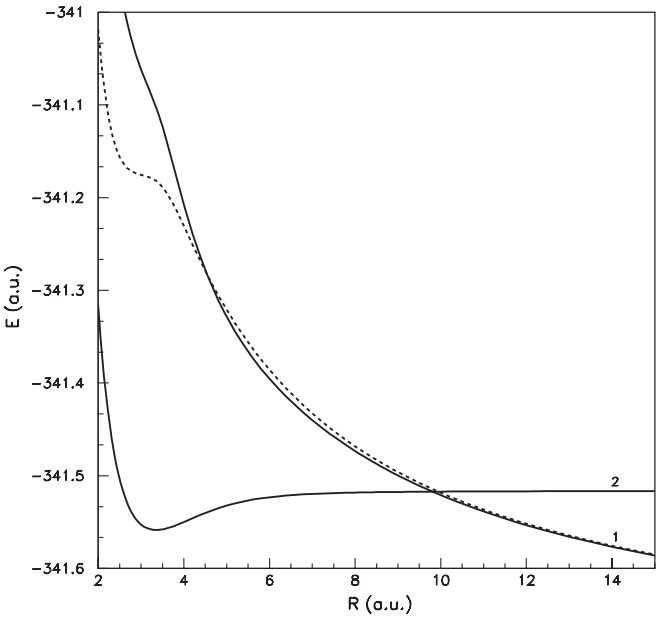


FIG. 1. Adiabatic potential-energy curves for the $P^{3+}(3s^2)^1S + He(1s^2)^1S$ system: $^1\Sigma^+$ states, solid lines; and $^1\Pi$ states, dashed lines. (1) $^1\Sigma^+$ and $^1\Pi$ states correlated to the $P^{2+}(3s^23p)^2P^o + He^+(1s)^2S$ configuration. (2) $^1\Sigma^+$ state correlated to the $P^{3+}(3s^2)^1S + He(1s^2)^1S$ configuration; entry channel.

high, at $R = 9.71$ a.u. and thus may induce a strong interaction between the entry channel and the $^1\Sigma^+\{P^{2+}(3s^23p)^2P^o + He^+(1s)^2S\}$ one-electron capture level. Such features may also be noticed on the rotational-coupling matrix elements, with a brutal decrease of the rotational coupling between the entry channel and the $^1\Pi\{P^{2+}(3s^23p)^2P^o + He^+(1s)^2S\}$ capture channel from 0.0 a.u. to $-1.0$ a.u. at $R = 9.71$ a.u. showing the change of configuration at the crossing point. Effectively, rotational couplings between $^1\Sigma^+$ and $^1\Pi$ levels are zero at long range for states corresponding to different configurations and reach a value of 1.0 a.u. (or $-1.0$ a.u.) for $^1\Sigma^+ - ^1\Pi$ states corresponding to the same configuration. Because the main exit channel may be correlated by means of rotational coupling, an effective rotational effect may be expected in this process.

The $P^{3+}(3s^2)^1S + H(1s)^2S$ system appears more complicated. In this case, the entry channel is of doublet spin symmetry and only doublet states have to be considered in the charge-transfer process because spin-orbit effects may be neglected in the collision-energy range of interest.

TABLE II. Comparison of asymptotic energy levels with experimental data (a.u.) for the $P^{3+}(3s^2)^1S + H$ system.

| Calculated configurations | MRCI calculation $^2\Sigma$ | MRCI calculations $^2\Pi$ | Experiment [12] |
|---|---|---|---|
| $P^{3+}(3s^2)^1S + H(1s)^2S(^2\Sigma^+)$ | 0.6048 | | 0.6084 |
| $P^{2+}(3s^24s)^2S + H^+(^2\Sigma^+)$ | 0.5347 | | 0.5352 |
| $P^{2+}(3s^23d)^2D + H^+(^2\Sigma^+, ^2\Pi)$ | 0.5343 | 0.5343 | 0.5308 |
| $P^{2+}(3s3p^2)^2P + H^+(^2\Sigma^-, ^2\Pi)$ | 0.4983 | 0.4983 | 0.4962 |
| $P^{2+}(3s3p^2)^2S + H^+(^2\Sigma^+)$ | 0.4528 | | 0.4548 |
| $P^{2+}(3s3p^2)^2D + H^+(^2\Sigma^+, ^2\Pi)$ | 0.3342 | 0.3342 | 0.3397 |
| $P^{2+}(3s^23p)^2P^o + H^+(^2\Sigma^+, ^2\Pi)$ | 0 | 0.0 | 0 |

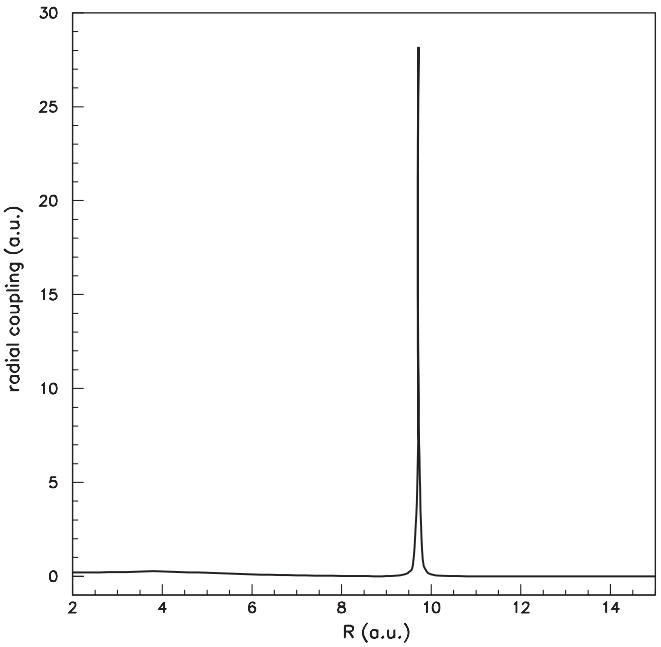


FIG. 2. Radial-coupling matrix elements between $^1\Sigma^+$ states of the $P^{3+}(3s^2)^1S + He(1s^2)^1S$ system.

Even if the first metastable ion $P^{3+}(3s3p)^3P^o$ leads to a $^2\Pi\{P^{3+}(3s3p)^3P^o + H\}$ entry channel, such a channel would be 8.47822 eV above the ground state, at an energy too high for this excited state to be populated. By taking into account the different excited states of the $P^{2+}$ ion, a number of molecular states may be involved in the charge-transfer process:

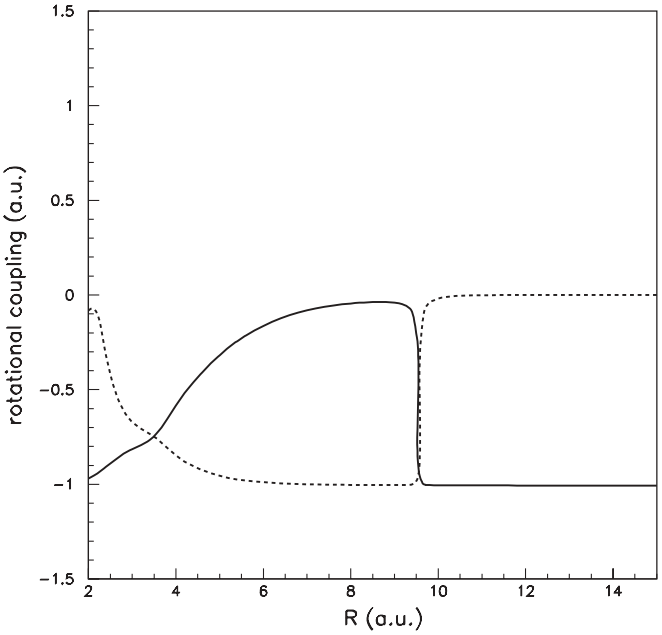


FIG. 3. Rotational-coupling matrix elements between $^1\Sigma^+$ and $^1\Pi$ states of the $P^{3+}(3s^2)^1S + He(1s^2)^1S$ system: $\langle(1)^1\Pi|iL_y|(1)^1\Sigma^+\rangle$, solid lines; and $\langle(1)^1\Pi|iL_y|(2)^1\Sigma^+\rangle$, dashed lines.

$P^{3+}(3s^2)^1S + H(1s)^2S \quad ^2\Sigma^+$ entry channel,
$P^{2+}(3s^24s)^2S + H^+ \quad ^2\Sigma^+$,
$P^{2+}(3s^23d)^2D + H^+ \quad ^2\Delta, ^2\Pi, ^2\Sigma^+$,
$P^{2+}(3s3p^2)^2P + H^+ \quad ^2\Pi, ^2\Sigma^-$,
$P^{2+}(3s3p^2)^2S + H^+ \quad ^2\Sigma^+$,
$P^{2+}(3s3p^2)^2D + H^+ \quad ^2\Delta, ^2\Pi, ^2\Sigma^+$,
$P^{2+}(3s^23p)^2P^o + H^+ \quad ^2\Pi, ^2\Sigma^+$.

With regard to asymptotical energy levels displayed in Table II, the $\{P^{2+}(3s^23d)^2D + H^+\}$ and $\{P^{2+}(3s^24s)^2S + H^+\}$ exit channels appear to lead to long-range avoided crossings with the entry channel, at internuclear distances of $R = 25.77$ a.u. and 27.32 a.u. respectively. Such long-range avoided crossings may be quasidiabatic and could not induce efficient charge transfer [16]. Thus, they have not been included in the calculation. The $\{P^{2+}(3s3p^2)^2P + H^+\}$ charge-transfer level, being of $^2\Sigma^-$ symmetry, cannot be correlated with the $\{P^{3+}(3s^2)^1S + H(1s)^2S\}^2\Sigma^+$ entry channel. The calculation has thus been performed for the four $^2\Sigma^+$ and two $^2\Pi$ states correlated to the entry channel and the $^2\Sigma^+\{P^{2+}(3s3p^2)^2S + H^+\}$; $^2\Sigma^+, ^2\Pi\{P^{2+}(3s3p^2)^2D + H^+\}$; and $^2\Sigma^+, ^2\Pi\{P^{2+}(3s^23p)^2P^o + H^+\}$ charge-transfer exit channels. The potential-energy curves are presented in Fig. 4. They show a very sharp avoided crossing around $R = 14$ a.u. between the entry channel and the $^2\Sigma^+\{P^{2+}(3s3p^2)^2S + H^+\}$ exit channel as well as an avoided crossing at shorter range, around $R = 8$ a.u. between the $^2\Sigma^+\{P^{2+}(3s3p^2)^2S + H^+\}$ and $^2\Sigma^+\{P^{2+}(3s3p^2)^2D + H^+\}$ charge-transfer channels. A smoother interaction may be also observed around $R = 4$ a.u., between the $^2\Sigma^+\{P^{2+}(3s3p^2)^2D + H^+\}$ and

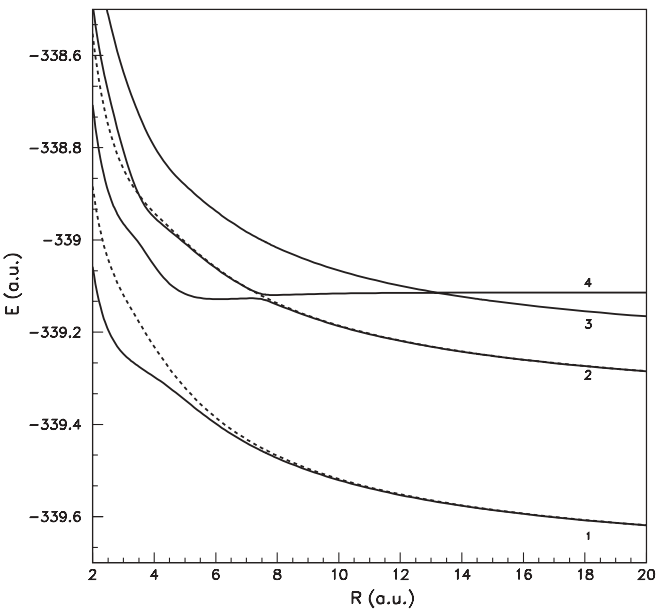


FIG. 4. Adiabatic potential-energy curves of the $P^{3+}(3s^2)^1S + H(1s)^2S$ system. $^2\Sigma^+$ states, solid lines; and $^2\Pi$ states, dashed lines. (1) $^2\Sigma^+$ and $^2\Pi$ states correlated to the $P^{2+}(3s^23p)^2P^o + H^+$ configuration. (2) $^2\Sigma^+$ and $^2\Pi$ states correlated to the $P^{2+}(3s3p^2)^2D + H^+$ configuration. (3) $^2\Sigma^+$ state correlated to the $P^{2+}(3s3p^2)^2S + H^+$ configuration. (4) $^2\Sigma^+$ state correlated to the $P^{3+}(3s^2)^1S + H(1s)^2S$ configuration; entry channel.

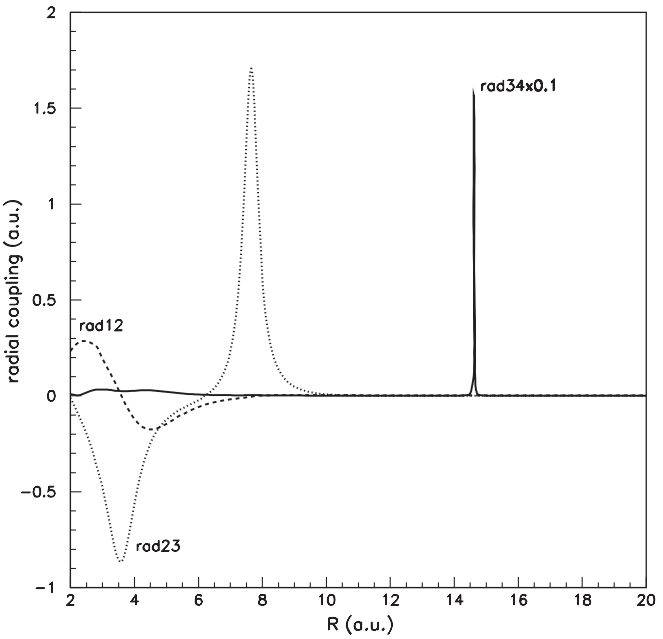


FIG. 5. Radial-coupling matrix elements between $^2\Sigma^+$ states of the $P^{3+}(3s^2)^1S + H(1s)^2S$ system.

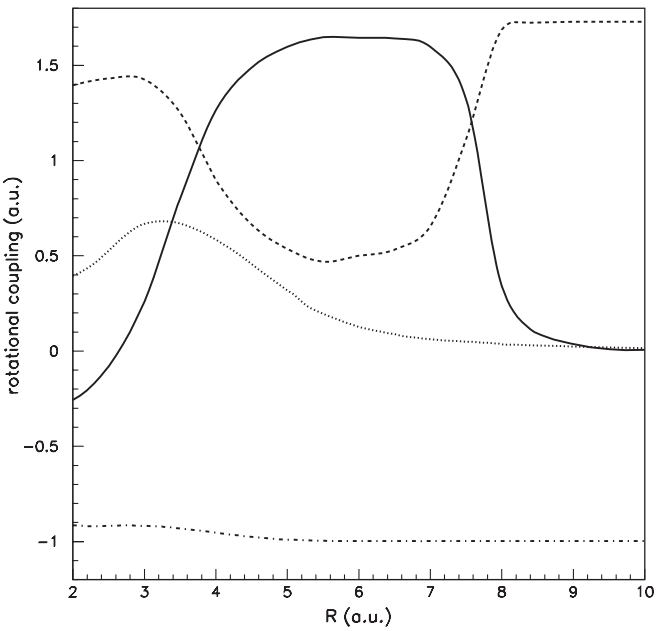


FIG. 6. Main features of the rotational-coupling matrix elements between $^2\Sigma^+$ and $^2\Pi$ states of the $P^{3+}(3s^2)^1S + H(1s)^2S$ system. $\langle(2)^2\Pi|iL_y|(3)^2\Sigma^+\rangle$, solid lines; $\langle(2)^2\Pi|iL_y|(2)^2\Sigma^+\rangle$, dashed lines; $\langle(2)^2\Pi|iL_y|(4)^2\Sigma^+\rangle$, dotted lines; and $\langle(1)^2\Pi|iL_y|(1)^2\Sigma^+\rangle$, dash-dotted lines.

$^2\Sigma^+\{P^{2+}(3s^23p)^2P^o + H^+\}$ states. No significant interaction may be pointed out between the $^2\Pi$ exit channels. The radial coupling matrix elements between $^2\Sigma^+$ levels presented in Fig. 5 show very peaked features corresponding to these avoided crossings. First, a very sharp peak, more than 15 a.u. high, at $R = 14.62$ a.u. between the entry channel and the $^2\Sigma^+\{P^{2+}(3s3p^2)^2S + H^+\}$ exit channel is related to the longer range avoided crossing already pointed out, and may induce a significant charge-transfer interaction. The other peak, 1.71 a.u. high, observed at $R = 7.65$ a.u. between the $^2\Sigma^+\{P^{2+}(3s3p^2)^2S + H^+\}$ and $^2\Sigma^+\{P^{2+}(3s3p^2)^2D + H^+\}$ molecular levels, is located in medium-range distance and could lead also to efficient charge transfer to the $^2\Sigma^+\{P^{2+}(3s3p^2)^2D + H^+\}$ state. In contrast, the radial-coupling matrix element between the $^2\Sigma^+\{P^{2+}(3s3p^2)^2D + H^+\}$ and $^2\Sigma^+\{P^{2+}(3s^23p)^2P^o + H^+\}$ levels is weak, about 0.2 a.u. high at the maximum, and the cross section on the lowest $^2\Sigma^+\{P^{2+}(3s^23p)^2P^o + H^+\}$ exit channel would certainly be small. Such features may also be observed on the rotational coupling matrix elements presented in Fig. 6. The avoided crossing between the $^2\Sigma^+\{P^{2+}(3s3p^2)^2S + H^+\}$ and $^2\Sigma^+\{P^{2+}(3s3p^2)^2D + H^+\}$ exit channels around $R =$ 8 a.u. is characterized by the strong decrease of the $\langle(2)^2\Pi|iL_y|(2)^2\Sigma^+\rangle$ rotational coupling in correspondence with the increase of the $\langle(2)^2\Pi|iL_y|(3)^2\Sigma^+\rangle$ one. Effectively, the $\langle(2)^2\Pi|iL_y|(3)^2\Sigma^+\rangle$ rotational coupling is equal to zero at long range as $(2)^2\Pi$ and $(3)^2\Sigma^+$ are not correlated to the same configuration; at the avoided crossing, the $(3)^2\Sigma^+$ states acquires the character of the $(2)^2\Pi$ exit channel and the rotational coupling increases. In contrast, there is almost no interaction between the $(1)^2\Sigma^+$ state and the entry channel, so the rotational coupling $\langle(1)^2\Pi|iL_y|(1)^2\Sigma^+\rangle$ corresponding to states of the same configuration remains close to 1.0 a.u. for all internuclear distances.

## III. COLLISION DYNAMICS

The collision dynamics has been studied in the 0.1–700-keV laboratory energy range by means of semiclassical methods, which are well adapted in this collision domain. Effectively, straight-line trajectories may be considered as satisfying collision energies greater than 10 eV/amu [17,18]. We have used the EIKONXS program [19] based on an efficient propagation method. Both radial-coupling and rotational-coupling matrix elements were taken into account, as well as translational effects using common translation factors as proposed by Errea *et al.* [14] in order to satisfy correct scattering-boundary conditions. The phosphorus nucleus has been taken as origin of the electronic coordinates.

For the $P^{3+}(3s^2)^1S + He$ collision system, the transition between the entry channel and the $^1\Sigma^+$ and $^1\Pi$ charge-transfer levels $\{P^{2+}(3s^23p)^2P^o + He^+(1s)^2S\}$ has to be considered. The results are presented in Table III and Fig. 7. The values of the cross sections present slight variations in a wide range of collision energies, between 0.1 and 20 keV, as well for the $\sigma_{21}^{\Sigma}$ cross section between the entry channel and the $^1\Sigma^+\{P^{2+}(3s^23p)^2P^o + He^+(1s)^2S\}$ level, than for the $\sigma_{21}^{\Pi}$ cross section toward the $^1\Pi\{P^{2+}(3s^23p)^2P^o + He^+(1s)^2S\}$ charge-transfer channel. As expected, in this energy domain, a significant charge transfer is observed between the entry channel and the $^1\Sigma^+\{P^{2+}(3s^23p)^2P^o + He^+(1s)^2S\}$ exit channel related to the strong radial-coupling matrix element between these states. In a wide energy range up to about 30 keV, the collision system is driven mainly by the radial coupling between the $^1\Sigma^+$ entry channel and the $^1\Sigma^+$ charge-transfer level. Such value of the cross-section reaches a maximum around $E_{\text{coll}} = 120$ keV and decreases significantly at higher energies. However, the value of the $\sigma_{21}^{\Pi}$ cross section

TABLE III. Total and partial cross sections between the different channels for the $P^{3+}(3s^2)^1S + He$ system (in $10^{-16}$ cm$^2$).

| $v$ (a.u.) | $E_{lab}$ (keV) | $\sigma_{21}^{\Sigma}$ $^1\Sigma^+$-$^1\Sigma^+$ | $\sigma_{21}^{\Pi}$ $^1\Sigma^+$-$^1\Pi$ | $\sigma_{tot}$ |
|---|---|---|---|---|
| 0.01 | 0.08 | 8.47 | 1.87 | 10.34 |
| 0.02 | 0.31 | 8.66 | 2.39 | 11.05 |
| 0.03 | 0.70 | 8.39 | 2.83 | 11.22 |
| 0.04 | 1.24 | 8.16 | 3.10 | 11.26 |
| 0.05 | 1.93 | 7.92 | 3.22 | 11.14 |
| 0.06 | 2.78 | 7.58 | 3.25 | 10.83 |
| 0.07 | 3.79 | 7.63 | 3.28 | 10.91 |
| 0.08 | 4.95 | 7.55 | 3.30 | 10.85 |
| 0.09 | 6.27 | 7.51 | 3.32 | 10.83 |
| 0.10 | 7.74 | 7.62 | 3.37 | 10.99 |
| 0.15 | 17.42 | 7.75 | 3.77 | 11.52 |
| 0.20 | 30.97 | 8.56 | 4.80 | 13.36 |
| 0.25 | 48.39 | 9.27 | 6.17 | 15.44 |
| 0.30 | 69.69 | 9.35 | 8.02 | 17.37 |
| 0.35 | 94.86 | 9.45 | 9.65 | 19.10 |
| 0.40 | 123.9 | 9.64 | 10.67 | 20.31 |
| 0.50 | 193.5 | 9.62 | 13.14 | 22.76 |
| 0.60 | 278.7 | 7.89 | 14.43 | 22.32 |
| 0.70 | 379.4 | 6.13 | 14.74 | 20.87 |
| 0.80 | 495.5 | 4.93 | 14.39 | 19.32 |
| 0.90 | 636.9 | 4.24 | 13.68 | 17.92 |
| 1.00 | 774.3 | 3.86 | 12.85 | 16.71 |

increases significantly at higher energies, which points out an important rotational effect for energies greater than 100 keV. Such a rotational effect was expected in a collision system where a rotational coupling interaction occurs directly between the entry channel and the main exit channel. Both radial and rotational interactions lead to a maximum of the total value

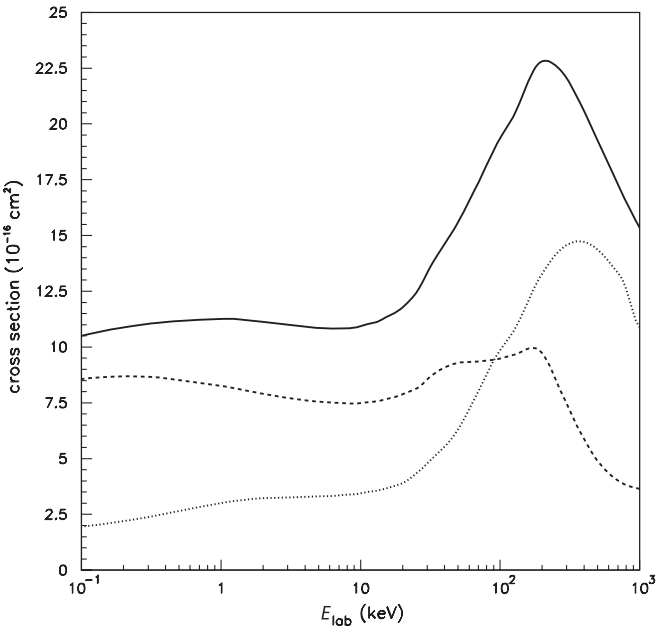


FIG. 7. Total and partial cross sections for the $P^{3+}(3s^2)^1S + He(1s^2)^1S$ collision system (in $10^{-16}$ cm$^2$): total cross section, solid lines; partial cross section on the $^1\Sigma^+$ exit channel $\sigma_{21}^{\Sigma}$; dashed lines; and partial cross section on the $^1\Pi$ exit channel $\sigma_{21}^{\Pi}$, dotted lines.

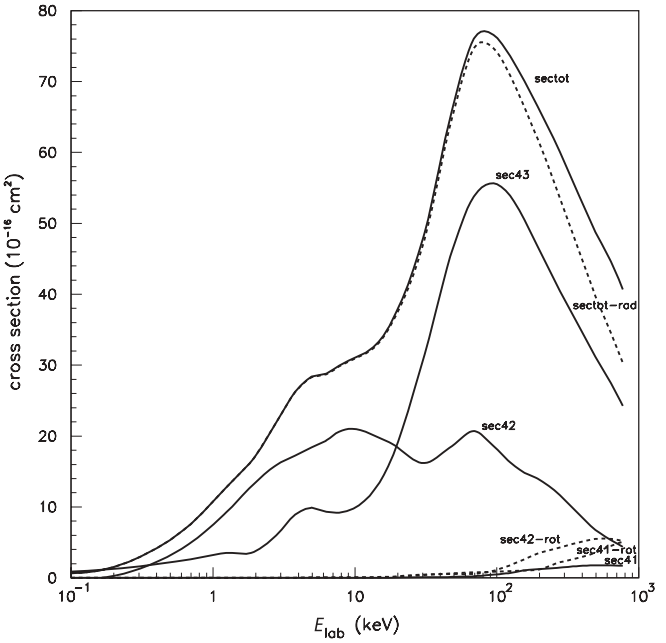


FIG. 8. Total and partial cross sections for the $P^{3+}(3s^2)^1S + H(1s)^2S$ collision system (in $10^{-16}$ cm$^2$). Total cross sections: "sectot" (solid lines), total cross section with radial and rotational coupling; and "sectot-rad" (dashed lines), total cross section with radial coupling only. Partial cross sections on $^2\Sigma^+$ states (solid lines): "sec43," $\sigma_{43}$ $^2\Sigma^+$-$^2\Sigma^+$; "sec42," $\sigma_{42}$ $^2\Sigma^+$-$^2\Sigma^+$; and "sec41," $\sigma_{41}$ $^2\Sigma^+$-$^2\Sigma^+$. Partial cross sections on $^2\Pi$ states (dashed lines): "sec42-rot," $\sigma_{42}$ $^2\Sigma^+$-$^2\Pi$; and "sec41-rot," $\sigma_{41}$ $^2\Sigma^+$-$^2\Pi$.

of the cross-section around $E_{lab} = 200$ keV, and then the total charge-transfer cross section significantly decreases at greater collision energies.

The values of the total and partial cross sections for the $P^{3+}(3s^2)^1S + H(1s)^2S$ collision system are presented in Table IV and Fig. 8. The total value of the cross-section presents a strong maximum around $E_{lab} = 100$ keV in relation mainly with the maximum of the value of the partial charge-transfer cross section on the $^2\Sigma^+\{P^{2+}(3s3p^2)^2S + H^+\}$ exit channel. As pointed out in the previous paragraph, the process is driven essentially by the very strong radial coupling between the entry channel and the $^2\Sigma^+\{P^{2+}(3s3p^2)^2S + H^+\}$ charge-transfer level. The corresponding $\sigma_{43}$ partial cross section accounts for more than 70% of the total cross section at the maximum. However, the peaked radial coupling with the $^2\Sigma^+\{P^{2+}(3s3p^2)^2D + H^+\}$ charge-transfer channel also provides a significant partial charge-transfer cross section, in particular at lower collision energies. As expected, the partial cross section value on the lowest $^2\Sigma^+\{P^{2+}(3s^23p)^2P^o + H^+\}$ exit channel remains very low with regard to the very smooth corresponding radial-coupling matrix element. In the present charge-transfer process, the rotational effect remains weak in the whole energy range compared to, for example, the $P^{3+}(3s^2)^1S + He$ collision system. Effectively, for the $P^{3+}(3s^2)^1S + H(1s)^2S$ collision system, the $^2\Sigma^+\{P^{2+}(3s3p^2)^2S + H^+\}$ exit channel, which presents the strongest interaction with the entry channel, cannot induce rotational effect. The rotational coupling may take

TABLE IV. Total and partial cross sections between the different channels for the $P^{3+}(3s^2)^1S + H$ system (in $10^{-16}$ cm$^2$).

| $v$ (a.u.) | $E_{lab}$ (keV) | $\sigma_{41}\ ^2\Sigma^+$-$^2\Sigma^+$ | $\sigma_{41}\ ^2\Sigma^+$-$^2\Pi$ | $\sigma_{42}\ ^2\Sigma^+$-$^2\Sigma^+$ | $\sigma_{42}\ ^2\Sigma^+$-$^2\Pi$ | $\sigma_{43}\ ^2\Sigma^+$-$^2\Sigma^+$ | $\sigma_{tot}$ |
|---|---|---|---|---|---|---|---|
| 0.01 | 0.08 | 0.0 | 0.0 | 0.01 | 0.0 | 0.77 | 0.78 |
| 0.02 | 0.31 | 0.0 | 0.0 | 1.33 | 0.0 | 1.63 | 2.96 |
| 0.03 | 0.70 | 0.0 | 0.0 | 4.95 | 0.0 | 2.62 | 7.57 |
| 0.04 | 1.24 | 0.0 | 0.01 | 9.24 | 0.0 | 3.51 | 12.76 |
| 0.05 | 1.93 | 0.0 | 0.01 | 13.22 | 0.0 | 3.64 | 16.87 |
| 0.06 | 2.78 | 0.0 | 0.01 | 15.91 | 0.02 | 5.99 | 21.93 |
| 0.07 | 3.79 | 0.0 | 0.03 | 17.25 | 0.03 | 8.93 | 26.24 |
| 0.08 | 4.95 | 0.0 | 0.04 | 18.40 | 0.05 | 9.89 | 28.38 |
| 0.09 | 6.27 | 0.0 | 0.04 | 19.38 | 0.06 | 9.34 | 28.82 |
| 0.10 | 7.74 | 0.0 | 0.04 | 20.63 | 0.07 | 9.19 | 29.93 |
| 0.15 | 17.42 | 0.02 | 0.10 | 19.14 | 0.16 | 16.05 | 35.47 |
| 0.20 | 30.97 | 0.08 | 0.40 | 16.20 | 0.48 | 31.51 | 48.67 |
| 0.25 | 48.39 | 0.13 | 0.62 | 18.61 | 0.53 | 46.12 | 66.01 |
| 0.30 | 69.69 | 0.23 | 0.78 | 20.68 | 0.57 | 53.93 | 76.19 |
| 0.35 | 94.86 | 0.46 | 0.88 | 18.60 | 1.00 | 55.64 | 76.58 |
| 0.40 | 123.9 | 0.69 | 0.97 | 16.29 | 1.78 | 53.89 | 73.62 |
| 0.50 | 193.5 | 1.21 | 1.14 | 13.99 | 3.41 | 46.75 | 66.50 |
| 0.60 | 278.7 | 1.44 | 2.20 | 11.67 | 4.29 | 40.45 | 60.05 |
| 0.70 | 379.4 | 1.68 | 2.84 | 8.94 | 4.99 | 35.47 | 53.92 |
| 0.80 | 495.5 | 1.77 | 3.56 | 6.76 | 5.49 | 31.19 | 48.77 |
| 0.90 | 636.9 | 1.75 | 4.53 | 5.32 | 5.48 | 27.46 | 44.58 |
| 1.00 | 774.3 | 1.72 | 5.11 | 4.36 | 5.22 | 24.26 | 40.67 |

place essentially by means of the interaction with the lower $^2\Pi\{P^{2+}(3s3p^2)^2D + H^+\}$ exit channel, after an initial interaction between the entry channel and the $^2\Sigma^+\{P^{2+}(3s3p^2)^2S + H^+\}$ exit channel. This mechanism cannot be as efficient as a direct interaction with the entry channel, and its effect remains small. A similar conclusion may be pointed out for the lowest $^2\Pi\{P^{2+}(3s^23p)^2P^o + H^+\}$ charge-transfer channel. The rotational effect is negligible for this collision system for energies less than 50 keV, and even for higher collision energies its effect is very weak.

These results may be compared to a previous work on the $P^{2+}(3s3p^2)^2P^o$ + H charge-transfer system [8]. In that case, $^{1,3}\Sigma^+$ and $^{1,3}\Pi$ entry channels have to be considered in the collision process, and statistical weights of the different entry channels have to be taken into account. This leads, of course, to a preponderant contribution of the triplet manifold, which accounts for three-quarters of the population of the entry channel. Anyway, some common general features may be pointed out for these three systems. As for the charge-transfer recombination of $P^{3+}(3s^2)^1S$ ions on atomic hydrogen and helium, the value of the total cross section presents a maximum at higher collision energies, around 50 keV for the $P^{2+}(3s3p^2)^2P^o + H$ charge-transfer system and around 100 keV and 200 keV for the $P^{3+}(3s^2)^1S + H$ and $P^{3+}(3s^2)^1S + He$ reactions, respectively. This maximum may be attributed essentially to a radial coupling interaction for the $P^{3+}(3s^2)^1S + H$ collision system. In contrast, it may be due mainly to an increasing rotational effect at higher collision energies for the $P^{3+}(3s^2)^1S + He$ and $P^{2+}(3s3p^2)^2P^o + H$ collision systems. Effectively, a significant rotational coupling effect may be noticed from the $^{1,3}\Pi$ entry channels of $P^{2+}(3s3p^2)^2P^o + H$, which may be evaluated to about 30% at the maximum. This appears less important than for the $P^{3+}(3s^2)^1S + He$ collision system, where the rotational effect may reach up to 60% for the total charge-transfer cross section, but such rotational-coupling interaction is essential for the description of the $P^{2+}(3s3p^2)^2P^o + H$ and $P^{3+}(3s^2)^1S + He$ collisions, contrary to the $P^{3+}(3s^2)^1S + H$ charge-transfer system, where it remains low.

## IV. CONCLUDING REMARKS

This work provides accurate molecular data, potential-energy curves, and radial- and rotational-coupling matrix elements for the $P^{3+}(3s^2)^1S + He(1s^2)^1S$ and $P^{3+}(3s^2)^1S + H(1s)^2S$ collision systems. A semiclassical collision treatment, taking account of all the states involved in the process, has been performed, and analysis of the radial- and rotational-coupling interactions has been developed for both collision systems and compared to the previous results for the $P^{2+}(3s3p^2)^2P^o + H$ charge-transfer reaction. General features may be pointed out with different rotational-coupling effects for these systems. Such collision results are essential in understanding fundamental processes involved in heavy-ion beams in order for them to be used in therapeutic applications.

[1] D. Péquignot, G. Stasinska, and S. M. V. Aldrovandi, Astron. Astrophys. **63**, 313 (1978).
[2] J. B. Kingdon and G. J. Ferland, Astrophys. J. **516**, L107 (1999).
[3] S. L. Baliunas and S. E. Butler, Astrophys. J. Lett. **235**, L45 (1980).
[4] S. R. Pottasch, J. Bernard-Salas, and T. L. Roellig, Astron. Astrophys. **481**, 393 (2008).
[5] V. Lebouteiller, Kuassivi, and R. Ferlet, Astron. Astrophys. **443**, 509 (2005).
[6] M. A. Pasek and D. S. Lauretta, Astrobiology **5**, 515 (2005).
[7] J.-P. Gu, G. Hirsch, R. J. Buenker, M. Kimura, C. M. Dutta, and P. Nordlander, Phys. Rev. A **59**, 405 (1999).
[8] M. C. Bacchus-Montabonel and Y. S. Tergiman, Chem. Phys. Lett. **422**, 122 (2006).
[9] J. B. Kingdon and G. J. Ferland, Astrophys. J. Suppl. Ser. **106**, 205 (1996).
[10] H. J. Werner and P. Knowles, MOLPRO package of *ab initio* programs.
[11] D. E. Woon and T. H. Dunning Jr., J. Chem. Phys. **98**, 1358 (1993).
[12] NIST Atomic Spectra Database levels data, http://physics.nist.gov/cgi-bin/AtData/main_asd
[13] M. C. Bacchus-Montabonel, R. Cimiraglia, and M. Persico, J. Phys. B **17**, 1931 (1984).
[14] L. F. Errea, L. Mendez, and A. Riera, J. Phys. B **15**, 101 (1982).
[15] M. C. Bacchus-Montabonel and P. Ceyzeriat, Phys. Rev. A **58**, 1162 (1998).
[16] P. Honvault, M. C. Bacchus-Montabonel, and R. McCarroll, J. Phys. B **27**, 3115 (1994).
[17] B. H. Bransden and M. R. C. McDowell, *Charge Exchange and the Theory of Ion-Atom Collisions* (Clarendon, Oxford, 1992), pp. 63–64.
[18] S. Kravis, H. Saitoh, K. Okuno, K. Soejima, M. Kimura, I. Shimamura, Y. Awaya, Y. Kaneko, M. Oura, and N. Shimakura, Phys. Rev. A **52**, 1206 (1995).
[19] R. J. Allan, C. Courbin, P. Salas, and P. Wahnon, J. Phys. B **23**, L461 (1990).